LITERATURE CITED

Breitbart AS, Grande DA, Mason JM, Barcia M, James T, Grant RT. 1999. Gene-enhanced tissue engineering: applications for bone healing using cultured periosteal cells transduced retrovirally with the BMP-7 gene. Ann Plast Surg 42:488-495.

Brinkhof B, Spee B, Rothuizen J, Penning LC. 2006. Development and evaluation of canine reference genes for accurate quantification of gene expression. Anal Biochem. 356:36-43.

Cheng SL, Lou J, Wright NM, Lai CF, Avioli LV, Riew KD. 2001. In vitro and in vivo induction of bone formation using a recombinant adenoviral vector carrying the human BMP-2 gene. Calcif Tissue Int 68:87-94.

Ducy P, Zhang R, Geoffroy V, Ridall AL, Karsenty G. 1997. Osf2/Cbfa1: a transcriptional activator of osteoblast differentiation. Cell 89:747-754.

Franceschi RT, Wang D, Krebsbach PH, Rutherford RB. 2000. Gene therapy for bone formation: in vitro and in vivo osteogenic activity of an adenovirus expressing BMP7. J Cell Biochem 78:476-486.

Gronthos S, Brahim J, Li W, Fisher LW, Cherman N, Boyde A, DenBesten P, Robey PG, Shi S. 2002. Stem cell properties of human dental pulp stem cells. J Dent Res 81:531-535.

Gronthos S, Mankani M, Brahim J, Robey PG, Shi S. 2000. Postnatal human dental pulp stem cells (DPSCs) in vitro and in vivo. Proc Natl Acad Sci U S A 97:13625-13630.

Gysin R, Wergedal JE, Sheng MH, Kasukawa Y, Miyakoshi N, Chen ST, Peng H, Lau KH, Mohan S, Baylink DJ. 2002. Ex vivo gene therapy with stromal cells transduced with a retroviral vector containing the BMP4 gene completely heals critical size calvarial defect in rats. Gene Ther 9:991-999.

Hiraga T, Ninomiya T, Hosoya A, Takahashi M, Nakamura H. 2009. Formation of bone-like mineralized matrix by periodontal ligament cells in vivo: a morphological study in rats. J Bone Miner Metab 27:149-157.

Hirata K, Mizuno A, Yamaguchi A. 2007. Transplantation of skin fibroblasts expressing BMP-2 contributes to the healing of critical-sized bone defects. J Bone Miner Metab 25:6-11.

Hirata K, Tsukazaki T, Kadowaki A, Furukawa K, Shibata Y, Moriishi T, Okubo Y, Bessho K, Komori T, Mizuno A, Yamaguchi A. 2003. Transplantation of skin fibroblasts expressing BMP-2 promotes bone repair more effectively than those expressing Runx2. Bone 32:502-512.

Hosoya A, Nakamura H, Ninomiya T, Hoshi K, Yoshiba K, Yoshiba N, Takahashi M, Okabe T, Sahara N, Yamada H, Kasahara E, Ozawa H. 2007. Hard tissue formation in subcutaneously transplanted rat dental pulp. J Dent Res 86:469-474.

Kadowaki A, Tsukazaki T, Hirata K, Shibata Y, Okubo Y, Bessho K, Komori T, Yoshida N, Yamaguchi A. 2004. Isolation and characterization of a mesenchymal cell line that differentiates into osteoblasts in response to BMP-2 from calvariae of GFP transgenic mice. Bone 34:993-1003.

Katagiri T, Yamaguchi A, Ikeda T, Yoshiki S, Wozney JM, Rosen V, Wang EA, Tanaka H, Omura S, Suda T. 1990. The non-osteogenic mouse pluripotent cell line, C3H10T1/2, is induced to differentiate into osteoblastic cells by recombinant human bone morphogenetic protein-2. Biochem Biophys Res Commun 172:295-299.

Katagiri T, Yamaguchi A, Komaki M, Abe E, Takahashi N, Ikeda T, Rosen V, Wozney JM, Fujisawa-Sehara A, Suda T. 1994. Bone morphogenetic protein-2 converts the differentiation pathway of C2C12 myoblasts into the osteoblast lineage. J Cell Biol 127:1755-1766.

Kawasaki K, Aihara M, Honmo J, Sakurai S, Fujimaki Y, Sakamoto K, Fujimaki E, Wozney JM, Yamaguchi A. 1998. Effects of recombinant human bone morphogenetic protein-2 on differentiation of cells isolated from human bone, muscle, and skin. BONE 23:223-231.

Komori T, Yagi H, Nomura S, Yamaguchi A, Sasaki K, Deguchi K, Shimizu Y, Bronson RT, Gao YH, Inada M, Sato M, Okamoto R, Kitamura Y, Yoshiki S, Kishimoto T. 1997. Targeted disruption of Cbfa1 results in a complete lack of bone formation owing to maturational arrest of osteoblasts. Cell 89:755-764.

Krebsbach PH, Gu K, Franceschi RT, Rutherford RB. 2000. Gene therapy-directed osteogenesis: BMP-7-transduced human fibroblasts form bone in vivo. Hum Gene Ther 11:1201-1210.

Lee JY, Musgrave D, Pelinkovic D, Fukushima K, Cummins J, Usas A, Robbins P, Fu FH, Huard J. 2001. Effect of bone morphogenetic protein-2-expressing muscle-derived cells on healing of critical-sized bone defects in mice. J Bone Joint Surg Am 83-A:1032-1039.

Lee JY, Peng H, Usas A, Musgrave D, Cummins J, Pelinkovic D, Jankowski R, Ziran B, Robbins P, Huard J. 2002. Enhancement of bone healing based on ex vivo gene therapy using human muscle-derived cells expressing bone morphogenetic protein 2. Hum Gene Ther 13:1201-1211.

Lee JY, Qu-Petersen Z, Cao B, Kimura S, Jankowski R, Cummins J, Usas A, Gates C, Robbins P, Wernig A, Huard J. 2000. Clonal isolation of muscle-derived cells capable of enhancing muscle regeneration and bone healing. J Cell Biol 150:1085-1100.

Musgrave DS, Bosch P, Lee JY, Pelinkovic D, Ghivizzani SC, Whalen J, Niyibizi C, Huard J. 2000. Ex vivo gene therapy to produce bone using different cell types. Clin Orthop Relat Res:290-305.

Musgrave DS, Pruchnic R, Bosch P, Ziran BH, Whalen J, Huard J. 2002. Human skeletal muscle cells in ex vivo gene therapy to deliver bone morphogenetic protein-2. J Bone Joint Surg Br 84:120-127.

Nakashima K, Zhou X, Kunkel G, Zhang Z, Deng JM, Behringer RR, de Crombrugghe B. 2002. The novel zinc finger-containing transcription factor osterix is required for osteoblast differentiation and bone formation. Cell 108:17-29.

Neff MW, Rine J. 2006. A fetching model organism. Cell 124:229-231.

Otaki S, Ueshima S, Shiraishi K, Sugiyama K, Hamada S, Yorimoto M, Matsuo O. 2007. Mesenchymal progenitor cells in adult human dental pulp and their ability to form bone when transplanted into immunocompromised mice. Cell Biol Int 31:1191-1197.

Otto F, Thornell AP, Crompton T, Denzèl A, Gilmour KC, Rosewell IR, Stamp GW, Beddington RS, Mundlos S, Olsen BR, Selby PB, Owen MJ. 1997. Cbfa1, a candidate gene for cleidocranial dysplasia syndrome, is essential for osteoblast differentiation and bone development. Cell 89:765-771.

Partridge K, Yang X, Clarke NM, Okubo Y, Bessho K, Sebald W, Howdle SM, Shakesheff KM, Oreffo RO. 2002. Adenoviral BMP-2 gene transfer in mesenchymal stem cells: in vitro and in vivo bone formation on biodegradable polymer scaffolds. Biochem Biophys Res Commun 292:144-152.

Pelinkovic D, Lee JY, Adachi N, Fu FH, Huard J. 2001. Muscle-based gene therapy and tissue engineering. Crit Rev Eukaryot Gene Expr 11:121-129.

Riew KD, Wright NM, Cheng S, Avioli LV, Lou J. 1998. Induction of bone formation using a recombinant adenoviral vector carrying the human BMP-2 gene in a rabbit spinal fusion model. Calcif Tissue Int 63:357-360.

Ryoo HM, Lee MH, Kim YJ. 2006. Critical molecular switches involved in BMP-2-induced osteogenic differentiation of mesenchymal cells. Gene 366:51-57.

Seo BM, Miura M, Gronthos S, Bartold PM, Batouli S, Brahim J, Young M, Robey PG, Wang CY, Shi S. 2004. Investigation of multipotent postnatal stem cells from

human periodontal ligament. Lancet 364:149-155.

Takahashi Y, Yamamoto M, Tabata Y. 2005. Osteogenic differentiation of mesenchymal stem cells in biodegradable sponges composed of gelatin and beta-tricalcium phosphate. Biomaterials 26:3587-3596.

Takayanagi H, Juji T, Miyazaki T, Iizuka H, Takahashi T, Isshiki M, Okada M, Tanaka Y, Koshihara Y, Oda H, Kurokawa T, Nakamura K, Tanaka S. 1999. Suppression of arthritic bone destruction by adenovirus-mediated csk gene transfer to synoviocytes and osteoclasts. J Clin Invest 104:137-146.

Tamura S, Kataoka H, Matsui Y, Shionoya Y, Ohno K, Michi KI, Takahashi K, Yamaguchi A. 2001. The effects of transplantation of osteoblastic cells with bone morphogenetic protein (BMP)/carrier complex on bone repair. Bone 29:169-175.

Turgeman G, Pittman DD, Müller R, Kurkalli BG, Zhou S, Pelled G, Peyser A, Zilberman Y, Moutsatsos IK, Gazit D. 2001. Engineered human mesenchymal stem cells: a novel platform for skeletal cell mediated gene therapy. J Gene Med 3:240-251.

Yamaguchi A, Ishizuya T, Kintou N, Wada Y, Katagiri T, Wozney JM, Rosen V, Yoshiki S. 1996. Effects of BMP-2, BMP-4, and BMP-6 on osteoblastic differentiation of bone marrow-derived stromal cell lines, ST2 and MC3T3-G2/PA6. Biochem Biophys Res Commun 220:366-371.

Yamaguchi A, Katagiri T, Ikeda T, Wozney JM, Rosen V, Wang EA, Kahn AJ, Suda T, Yoshiki S. 1991. Recombinant human bone morphogenetic protein-2 stimulates osteoblastic maturation and inhibits myogenic differentiation in vitro. J Cell Biol 113:681-687.

Yamaguchi A, Komori T, Suda T. 2000. Regulation of osteoblast differentiation mediated by bone morphogenetic proteins, hedgehogs, and Cbfa1. Endocr Rev 21:393-411.

Wada Y, Kataoka H, Yokose S, Ishizuya T, Miyazono K, Gao YH, Shibasaki Y, Yamaguchi A. 1998. Changes in osteoblast phenotype during differentiation of enzymatically isolated rat calvaria cells. Bone 22:479-85.

FIGURE LEGENDS

Figure 1

A: Fibroblasts isolated from canine buccal mucosa (COFs). These cells show spindle-shaped cytoplasm with elongated nuclei. Numerous cultured cells expressed GFP signals under the fluorescence microscopic observation. B: Localization of GFP-positive COFs in GS-β/COFs complex before transplantation. GFP-positive COFs (white arrows) are observed in the GS-β/COFs complex. GS-β (pink asterisks) shows strong fluorescence. Bars: 50μm in A and B.

Figure 2

A: Effects of rhBMP-2 on ALP activity in COFs. The cells were cultured for 3days with various concentrations of rhBMP-2, and ALP activity was measured as described in Materials and Methods. *p<0.05. B-G: Effects of rhBMP-2 on histochemical detection of ALP in COFs. The cells were cultured for 6 days with various concentrations of rhBMP-2, and they were processed for histochemical staining of ALP as described in Materials and Methods. Concentrations of rhBMP-2: B; 0 ng/ml (control), C; 1 ng/ml, D; 50 ng/ml, E; 100 ng/ml, F; 250 ng/ml, G; 500 ng/ml.

Figure 3

Effects of rhBMP-2 on mRNA expression of *Runx2* (A), *Osterix*(B), and *Osteocalcin* (*OCN*) (C) in COFs. The cells were cultured for 3 or 6 days with or without rhBMP-2 (500 ng/ml), and mRNA expression was determined as described in Materials and Methods. Relative expression level of each mRNA shown in Figure 3 was normalized

to β-2-microglobulin mRNA. *p<0.05, **p<0.01(n=3).

Figure 4

Soft x-ray features of the transplanted complexes. A: 1 week after transplantation of control complex (GS-β/COFs). B: 1 week after transplantation of GS-β/BMP-2/COFs. C: 2 weeks after transplantation of control complex (GS-β/COFs). D: 2 weeks after transplantation of GS-β/BMP-2/COFs. E: 2 weeks after transplantation of GS-β/BMP-2.

Figure 5

Histology of transplanted complexes. A-F and H are undecalcified sections and G is decalcified paraffin section prepared as described in Materials and Methods. A: Histology of transplanted control complex (GS-β/COFs) after 1 week of the transplantation. Note that mineralized GS-β (brown to black) and non-mineralized GS-β (pink) are observed, but no ALP-positive cells are observed. B: Histology of transplanted GS-β/BMP-2/COFs complex after 1 week of the transplantation. Note that ALP-positive cells (blue) are observed around mineralized GS-β/bone (brown to black). C, D: Histology of transplanted GS-β/BMP-2 complex after 2 weeks of the transplantation. ALP-positive cells (blue) are observed around mineralized bone (brown to black). D is a higher magnification of C. E, F: Histology of transplanted GS-β/BMP-2/COFs complex after 2 weeks of the transplantation. Note that Numerous ALP-positive cells (blue) are observed around mineralized bone (brown to black). G: Histology of decalcified section of the transplanted GS-β/BMP-2/COFs complex after 2 weeks of the transplantation. Numerous osteocytes are embedded in bone matrices. Hematoxylin and eosin stain. H, I: Cartilage appeared in the transplants of GS-β/BMP-2

complex (H) and GS-β/BMP-2/COFs complex (I) after 2 weeks of the transplantation. Alcian blue stain. Bars: 100μm in A, B, C and E, 50 μm in E, 25 μm in D, F, G, H and I.

Figure 6

Localization of ALP-positive cells and GFP-positive cells in the ectopically formed bones at 2 weeks after transplantation of GS-β/BMP-2/COFs complex. GFP-positive cells were monitored before staining both ALP and von Kossa. Blue cells in A and C are ALP-positive cells, and mineralized bone is shown in brown. Pictures of B and D were taken by fluorescence microscope. Green cells in B and D are GFP-positive cells. Red arrows indicate the cells showing both positive for ALP and GFP, and yellow arrows indicate the cells showing GFP-positive but ALP-negative. Pink asterisks indicate the rests of GS-β. Bars indicate 20μm.

Figure 1

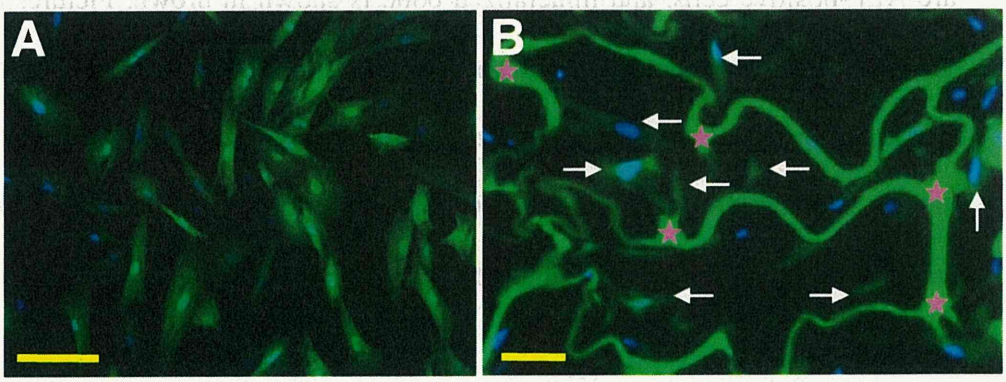

Figure 2

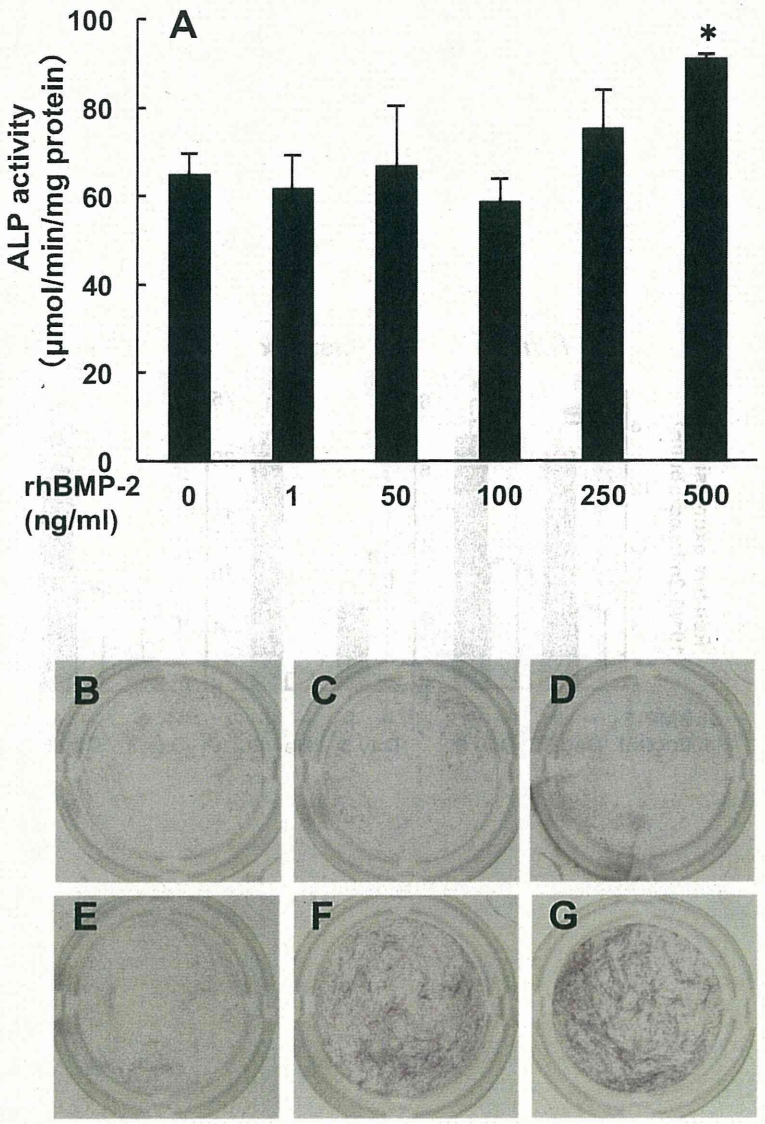
A
100
80
60
40
20
0
ALP activity
(μmol/min/mg protein)
*
rhBMP-2
(ng/ml)
0
1
50
100
250
500
B
C
D
E
F
G

Figure 3

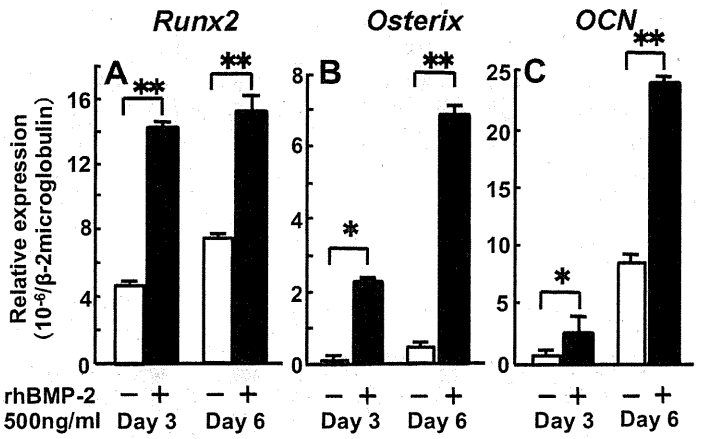
Runx2
Osterix
OCN
A
B
C
**
*
Relative expression
(10⁻⁶/β-2microglobulin)
0
4
8
12
16
2
6
20
25
10
15
5
rhBMP-2
500ng/ml
− +
Day 3
Day 6

Figure 4

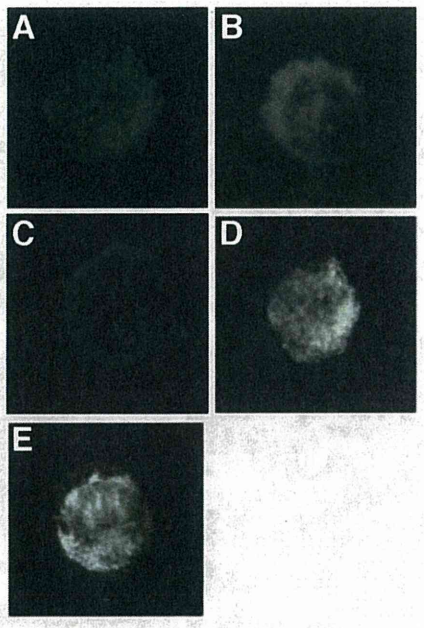

Figure 5

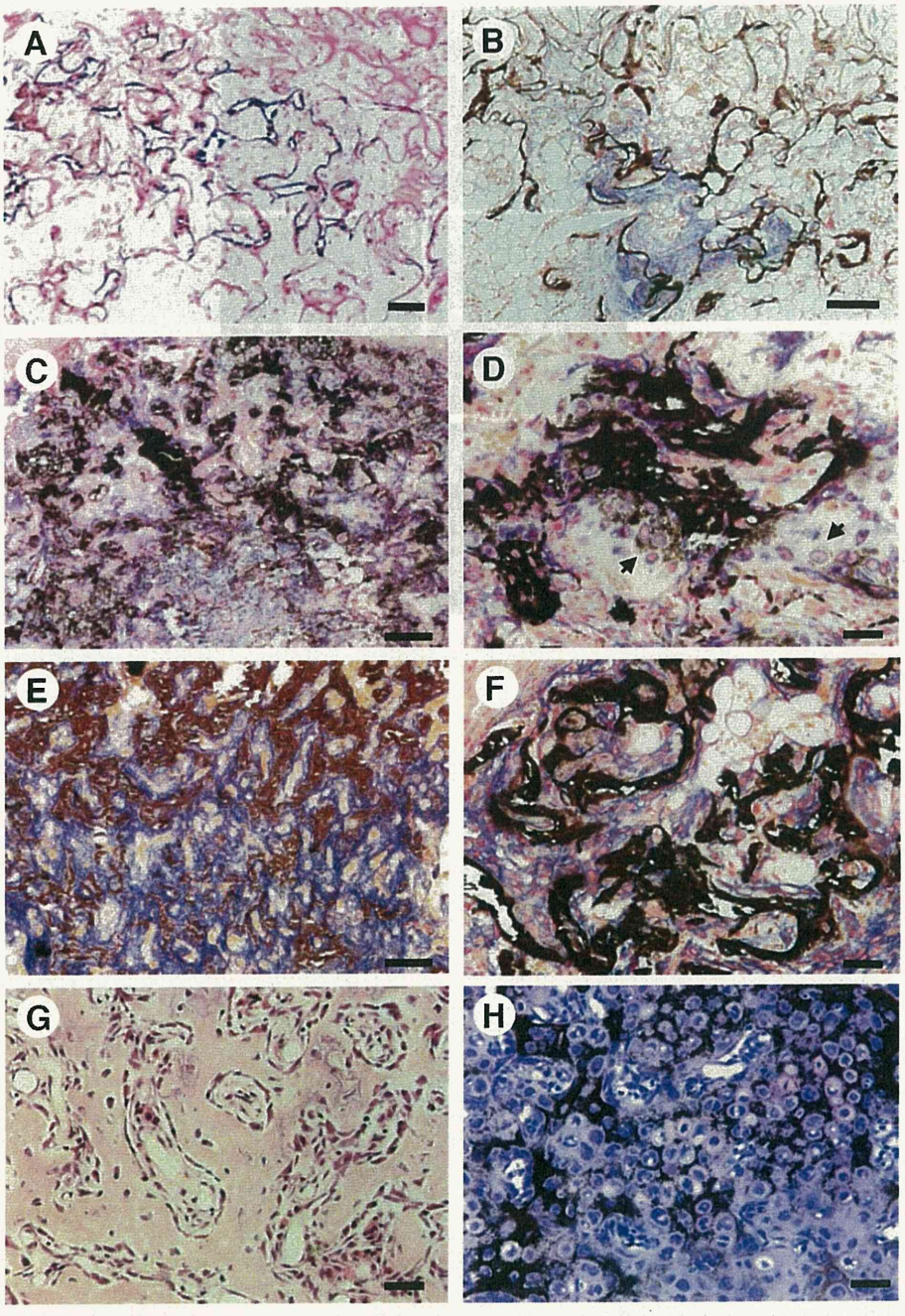

Figure 6

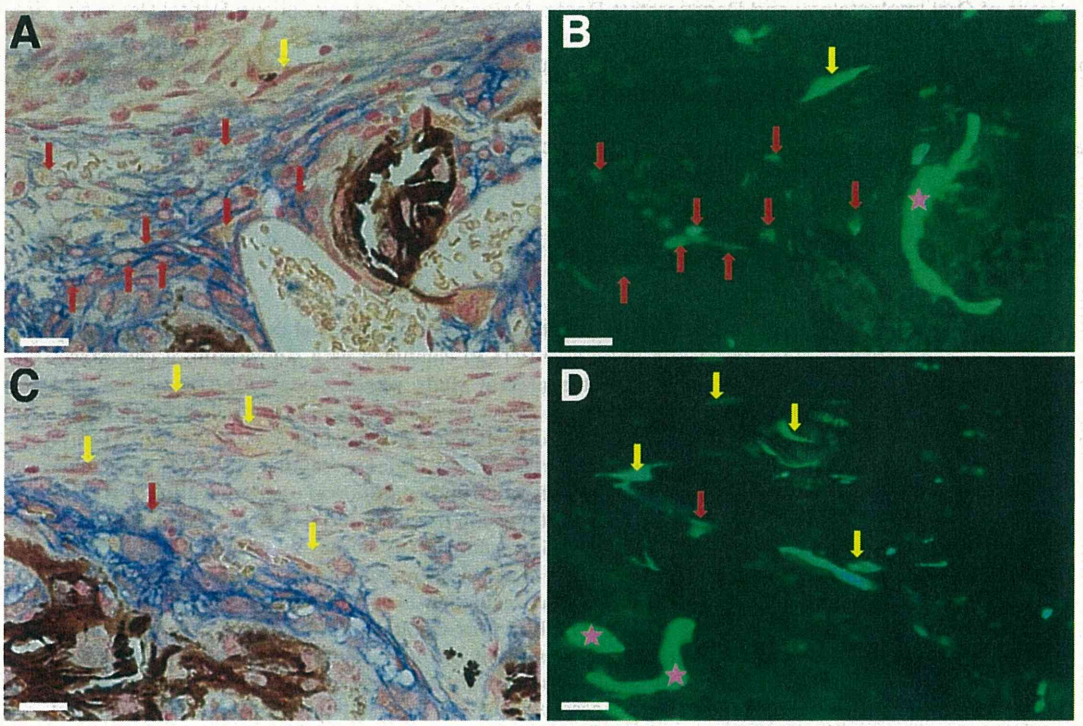

Molecular and Tissue Responses in the Healing of Rat Calvarial Defects After Local Application of Simvastatin Combined With Alpha Tricalcium Phosphate

Myat Nyan,[1,2,3] Takayuki Miyahara,[1,2] Kanako Noritake,[1,2] Jia Hao,[1,2] Reena Rodriguez,[1,2] Shinji Kuroda,[1] Shohei Kasugai[1,2]

[1] Department of Oral Implantology and Regenerative Dental Medicine, Tokyo Medical and Dental University, Tokyo, Japan

[2] Global Center of Excellence Program, International Research Center for Molecular Science in Tooth and Bone Diseases, Tokyo Medical and Dental University, Tokyo, Japan

[3] Department of Prosthodontics, University of Dental Medicine, Yangon, Myanmar

Received 29 May 2009; revised 20 August 2009; accepted 27 September 2009
Published online 18 December 2009 in Wiley InterScience (www.interscience.wiley.com). DOI: 10.1002/jbm.b.31559

Abstract: We have previously reported that healing of rat calvarial defects was enhanced by application of alpha tricalcium phosphate (αTCP) combined with simvastatin, a cholesterol synthesis inhibitor. The purpose of the present study was to investigate the cellular and molecular mechanisms in this phenomenon. Rat calvarial defects were grafted with αTCP with or without simvastatin or left untreated. Animals were sacrificed on 3, 7, 10, 14, and 21 days postoperatively and histological changes in the defect region were assessed. Gene expression patterns were examined by RT-PCR. Proliferation and migration of osteoprogenitor cells from the dura mater were increased in simvastatin group from day 3 to day 10 ($p < 0.01$). New bone formation was significantly increased in simvastatin group on day 14 and day 21 ($p < 0.01$). BMP-2 expression was significantly higher in simvastatin group on day 3 and day 14 ($p < 0.05$) and maintained until day 21. Increased upregulation of TGF-β1 was also observed in the simvastatin group on day 7 ($p < 0.05$) which was maintained until day 14. These findings suggest that the proliferation and recruitment of osteoprogenitor cells were critical steps in early stage of bone healing and that these steps were enhanced by TGF-β1 and BMP-2, which were stimulated by simvastatin. © 2009 Wiley Periodicals, Inc. J Biomed Mater Res Part B: Appl Biomater 93B: 65–73, 2010

Keywords: bone healing; simvastatin; alpha tricalcium phosphate; BMP-2; TGF-β; bone formation

INTRODUCTION

For regeneration of defective or lost bone tissue, various techniques for tissue engineering have been introduced. *In situ* bone regeneration therapy is one of them in which osteoconductive scaffolds combined with bioactive molecules are applied to stimulate the local host cells to upregulate osteoblastic differentiation and subsequent bone formation. Bone morphogenetic proteins (BMPs) are promising candidates for this approach of tissue engineering; however, there are still some problems to be solved for clinical application.[1] Simvastatin is one of the most commonly prescribed cholesterol lowering drugs, which has been shown to stimulate expression of BMP-2 *in vitro* and promote bone formation *in vivo*.[2] Recently, many research works have been emphasized on the local application of statins for *in situ* bone regeneration and repair.[3–16] We have also reported in our previous study that optimal dose of simvastatin combined with alpha tricalcium phosphate (αTCP) stimulated bone regeneration in the calvarial osteotomy defects in rats.[17] The objective of the present study was to investigate the molecular and cellular mechanisms in the early stage of bone healing by the application of simvastatin-αTCP combination in the rat calvarial defects.

MATERIALS AND METHODS

Sample Preparation and Measurement of *In Vitro* Drug Release

αTCP particles (Advance Co., Tokyo, Japan) having 500–700 μm in diameter and porous structure (mean pore size

Correspondence to: M. Nyan (e-mail: myatnyan@gmail.com)
Contract grant sponsors: Global Center of Excellence Program, International Research Center for Molecular Science in Tooth and Bone Diseases, Tokyo Medical and Dental University, Tokyo, Japan

~5 μm, mean porosity ~27%) were used. The samples were prepared according to the methods previously described.[17] Simvastatin (OHARA Pharmaceutical Co. Ltd., Koka, Shiga, Japan) was dissolved in ethanol and the solution was applied to the αTCP particles by dropping under sterile conditions. Ethanol was dried out completely in a laminar flow hood. Each sample was composed of 0.1 mg simvastatin combined with 14 mg αTCP particles. This dose was determined as the optimal dose for combining with αTCP to stimulate bone regeneration in the previous study. The loading efficacy was determined by dividing the retained amount of simvastatin by the initial loaded simvastatin concentration multiplied by 100%.

The release of simvastatin was measured using a UV-Visible spectrophotometer, Nanodrop, ND-1000 (NanoDrop Technologies, Wilmington). The spectrometer was calibrated using 6 standards of simvastatin solution at 37°C. The absorbance was measured at 238 nm and working curve for calculation of simvastatin concentrations was established from the absorbance values. The samples were placed in 500 μL of 0.1*M* tris buffer solution (pH 7.4), and positioned in an Taitec Personal 11 Shaker (Taitec Corp., Tokyo, Japan) set at 100 rpm and 37°C. The amount of drug released into the tris buffer was measured 24 hr after the initial immersion, then every day for 14 days. The cumulative concentration was calculated using the previously determined working curve.

Animal Procedures

The animal experiment protocol was approved by the institutional committee for animal experiments. Bilateral parietal bone defects were created according to the method previously reported. Male Wistar rats (16 weeks old) were anesthetized with a combination of ketamine-xylazine (40 and 5 mg/kg). The dorsal part of the cranium was shaved and prepared aseptically for surgery. A 20-mm long incision in the scalp along the sagittal suture was made, and the skin, subcutaneous tissue and periosteum were reflected, exposing the parietal bones. Two full-thickness bone defects of 5 mm diameter were trephined in the dorsal part of the parietal bone lateral to the sagittal suture. A 5-mm trephine bur was used to create the defects under constant irrigation with sterile physiologic solution to prevent overheating of the bone edges. Care was taken during the surgical procedure to prevent damage to dura mater. In TCP group, each defect was filled with 14 mg of αTCP (30 rats) and in simvastatin group, with 14 mg of simvastatin-αTCP combination (30 rats). In 30 animals, both defects were left unfilled to serve as control group.

Histological Observation

For histological observations, three rats from each group were sacrificed at 3, 7, 10, 14, and 21 days after surgery. The specimens were fixed in 10% neutralized formalin for 1 week, decalcified in EDTA for 4 weeks, and then embedded in paraffin. Coronal sections of about 5 μm thickness were cut, stained with haematoxylin-eosin and observed under an optical microscope (Biozero, Keyence, Tokyo, Japan). The image analysis was performed by using a computer-based image analyzing software (Image J, NIH) to measure the cell density and to quantify the newly formed bone area within the defect. The cell counter tool in the Image J software was applied to count the number of osteoprogenitor-like cells by clicking on the image of each cell manually after these cells were visually determined according to their morphology. The cell counter tool marked the counted cells so that repeated counting was avoided. The bone fill percentage (%) was calculated from the values of total defect area and area of newly formed bone.

Real-Time PCR Analysis

For gene expression analysis, three rats from each group were sacrificed at 3, 7, 10, 14, and 21 days after surgery. Two bone samples incorporating the individual defect region were obtained from parietal bones of each rat. Total RNA was extracted from the bone samples by using Trizol Reagent (Invitrogen, Carlsbad, CA). Complementary DNAs (cDNAs) were synthesized using a commercial kit (Superscript III First-Strand Synthesis Supermix, Invitrogen) according to the manufacturer's recommendations. Oligonucleotide primers were designed for amplification of messenger RNA (mRNA) encoding the following genes: ratGAPDH (forward: 5′-AACTCCCATTCTTCCACCTT-3′, reverse: 3′AGGGCCTCTCTCTTGCTCT-5′), ratBMP-2 (forward: 5′-AAGGCACCCTTTGTATGTGG-3′, reverse: 3′-CATGCCTTAGGGATTTTGGA-5′), ratTGF-beta1 (forward: 5′-CAACAATTCCTGGCGTTACC-3′, reverse: 3′-TGGGACTGATCCCATTGATT-5′) and ratVEGF (forward: 5′-TTGAGACCCTGGTGGACATC-3′, reverse: 3′-CTCCT-ATGTGCTGGCTTTGG-5′).

Real-time PCR quantification was performed with SYBR green PCR master-mix (Applied Biosystems) on an Applied Biosystems 7300 Real Time PCR System (ABI, Foster City, CA). Expression levels were determined using the relative threshold cycle (C_T) method as described by the manufacturer of the detection system. Expression levels were stated in terms of fold increase or decrease relative to un-operated normal rats of the same age. This was calculated for each gene by evaluating the expression $2^{-\Delta\Delta C_T}$, where $\Delta\Delta C_T$ is the result of subtracting $[C_{T\text{gene}} - C_{T\text{GAPDH}}]_{(\text{unoperated calibrator})}$ from $[C_{T\text{gene}} - C_{T\text{GAPDH}}]_{(\text{experimental group})}$.

Statistical Analysis

Data were firstly analyzed by one-way ANOVA. When this analysis suggested a significant difference between groups ($p < 0.05$), the data were further analyzed by Tukey *post hoc* multiple comparison tests.

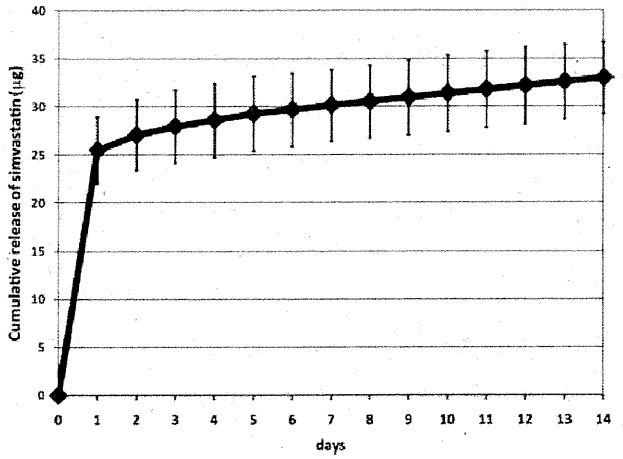

Figure 1. *In vitro* release pattern of simvastatin from αTCP. Values were shown as mean ± SD, $n = 5$.

RESULTS

In Vitro Release Behavior of Simvastatin From Alpha-Tricalcium Phosphate

The observed drug loading efficacy of αTCP for simvastatin was 93.4 ± 5.8%. Approximately 25% of adsorbed simvastatin was released after 24 hr. This initial burst release was followed by the gradual and stable release of the drug that was maintained until 2 weeks (Figure 1).

Histological Features

At day 3 after surgery, a significant thickening of dura mater was observed in simvastatin- αTCP combination group at the bone edges as well as in the middle of the defect. Round or cuboidal cells resembling undifferentiated mesenchymal cells and some osteoprogenitor-like cells migrated from dura mater to the area between the αTCP particles and dura mater. Some of these cells were also observed in the pores at the periphery of the particles which were located adjacent to the dura mater surface [Figure 2(c)]. On the other hand, control group showed the proliferation and migration of bone marrow mesenchymal cells from the bone edges and osteogenic cells from the periosteum over the bone edges. The middle of the defect was filled with connective tissue. Both control group and TCP group showed less extent of dura mater thickening and cell migration than simvastatin-αTCP combination group [Figure 2(a,b)].

At day 7, cell density became increased associated with formation of blood vessels in all groups. The cellular migration became more extensive in simvastatin-αTCP combination group at the center of the defect as well as near the bone edges. These cells took the morphology of proliferating preosteoblasts and recruited between αTCP particles and in the space between αTCP and bone edges. In some places, the cells resembling active osteoblasts condensed and began to lay down bone matrix [Figure 3(c,d)]. In the control group, the cellular proliferation was seen only at the bone edges whereas TCP group showed cell migration from dura mater at the middle of defect [Figure 3(a,b)].

At day 10, the osteogenic cells recruited between the TCP particles resembling preosteoblasts continued proliferation and migrating around the periphery of TCP particles. Some of these cells became differentiated into osteoblasts and began to lay down bone matrix in the simvastatin-αTCP combination group [Figure 4(c,d)]. Cell migration continued into the inner portion of TCP particles in both TCP and simvastatin-αTCP combination groups while many blood vessels were formed around the TCP particles [Figure 4(b,c)]. In the control group, the recruited cells at the bone edges differentiated into osteoblasts and began to form new bone [Figure 4(a)]. Cellular migration and proliferation were significantly higher in simvastatin-αTCP combination group at day 3 to day 10 ($p < 0.01$) (Figure 5).

At day 14, osteoblast differentiation and bone formation became extensive in the simvastatin-αTCP combination group so that the area between the αTCP particles became filled with newly formed bone. Active osteoblasts lined on this newly formed bone surface. The cells inside the αTCP particles also differentiated into osteoblasts and secreted bone matrix in this group [Figure 6(c)]. The cells recruited between αTCP particles in αTCP group also began to differentiate and synthesize bone matrix [Figure 6(b)]. In the control group, osteoblasts continued to form thin layer of new bone toward the center of the defect [Figure 6(a)].

At day 21, in simvastatin group, osteogenic cell migration and recruitment continued at many places eventually invading into the middle of the αTCP particles. New bone deposition was observed in the middle of the αTCP particles which were almost completely surrounded by the regenerated bone. Some parts of this new bone in contact with αTCP particles become mature and formed marrow spaces. New bone extensively replaced the αTCP particles which were located close to dura mater [Figure 7(c)]. In αTCP group, new bone was formed in the spaces between some particles but not as extensively as simvastatin group [Figure 7(b)]. In control group, osteoblasts lining along the newly formed bone surface became flattened and the center of the defect was filled with connective tissue [Figure 7(a)]. The percentage of new bone area was significantly higher in simvastatin-αTCP combination group at day 14 and day 21 ($p < 0.01$) (Figure 8).

Gene Expression Profiles

Gene expression experiments were conducted to investigate whether increased cellular proliferation and recruitment and augmented bone regeneration could be linked to TGF-β, BMP-2, and VEGF. All groups showed increased expression of TGF-β1 and BMP-2 from day 3 to 21. In simvastatin group, BMP-2 was upregulated since day 3 at a higher level than other groups ($p < 0.05$). All groups showed sim-

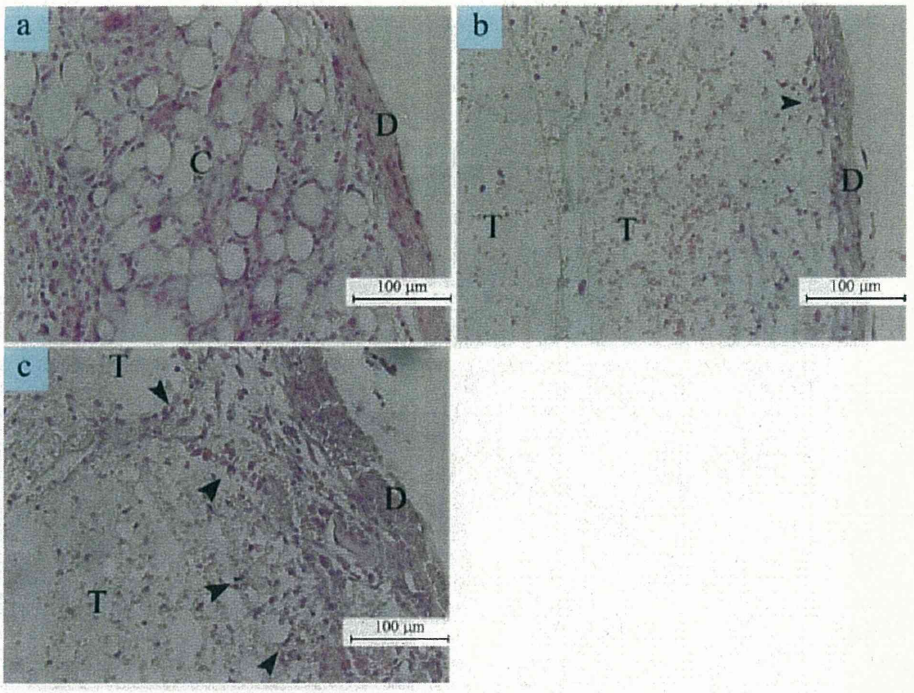

Figure 2. Photomicrographs of the calvarial defects at day 3 representing middle of the bone defects of (a) control (b) TCP and (c) simvastatin-αTCP combination groups. Arrow heads denote migrating osteogenic cells. D, dura mater; T, αTCP particles; C, connective tissue. [Color figure can be viewed in the online issue, which is available at www.interscience.wiley.com.]

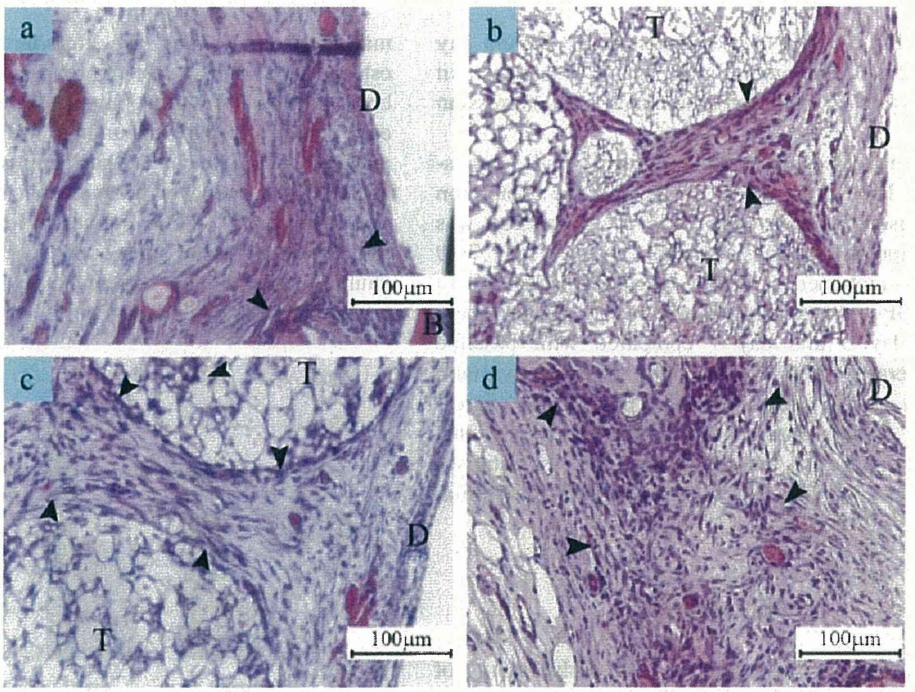

Figure 3. Photomicrographs of the calvarial defects at day 7 representing middle of the bone defects of (b) TCP and (c) simvastatin-αTCP combination groups. Panel (a) and (d) show control and simvastatin-αTCP combination groups near the bone edge. Arrow heads denote proliferating pre-osteoblasts. D, dura mater; T, αTCP particles; B, old bone. [Color figure can be viewed in the online issue, which is available at www.interscience.wiley.com.]

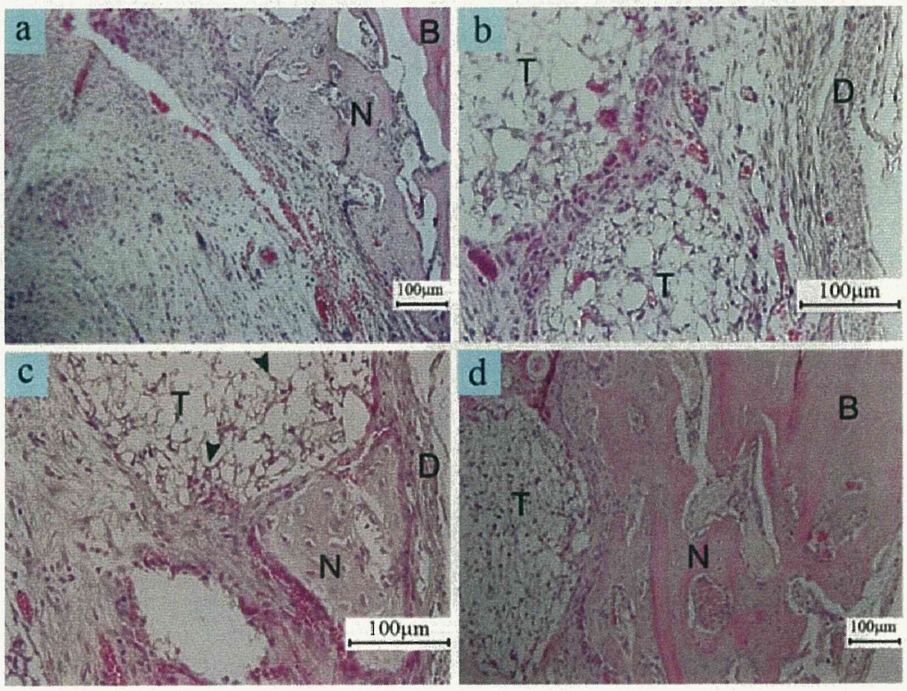

Figure 4. Photomicrographs of the calvarial defects at day 10 representing middle of the bone defects of (b) TCP and (c) simvastatin-αTCP combination groups. Panel (a) and (d) show control and simvastatin-αTCP combination groups near the bone edge. Arrow heads denote osteogenic cells migrating into αTCP particle. D, dura mater; T, αTCP particles; B, old bone; N, newly formed bone. [Color figure can be viewed in the online issue, which is available at www.interscience.wiley.com.]

ilar levels of BMP-2 mRNA expression at day 7 and day 10. The expression became higher again in simvastatin group at day 14 ($p < 0.05$) and maintained high expression until day 21.

All groups revealed slight increase in TGF-β1 expression at day 3. Then, from day 7 till day 21, the expression became increased in all groups. TGF-β1 expression was dramatically upregulated in simvastatin group at day 7 ($p < 0.05$) and maintained at higher levels until day 14. In contrast, VEGF mRNA expressions in all groups were increased at day 3 and day 7 compared with baseline (normal unoperated rats). At day 10 and 14, simvastatin group showed higher expressions of VEGF while expression levels in other groups tended to decrease toward the baseline level. However, the differences were not statistically significant. At day 21, all groups showed similar expression level (Figure 9).

DISCUSSION

Molecular and cellular mechanisms in the early healing of rat calvarial defects after local application of simvastatin-αTCP combination were examined in this study.

We found increased proliferation and migration of the osteogenic cells mainly from dura mater and also from bone edges in simvastatin group at the initial stage of healing (day 3, 7, and 10). During bone healing, the mesenchymal stem cells play an important role providing the osteogenic cells. The potential sources of stem cells are the bone marrow, the granulation tissue, the periosteum, the endosteum, and the surrounding soft tissues.[18,19] The dura mater is a component of the meninges, a group of fibrous connective tissues which function to protect both the brain and spinal cord.[20] Many studies have demonstrated that the initial patterning and subsequent regeneration of the cranial vault is regulated by secreted cytokines and donated precursor cells from the dura mater.[21–24]

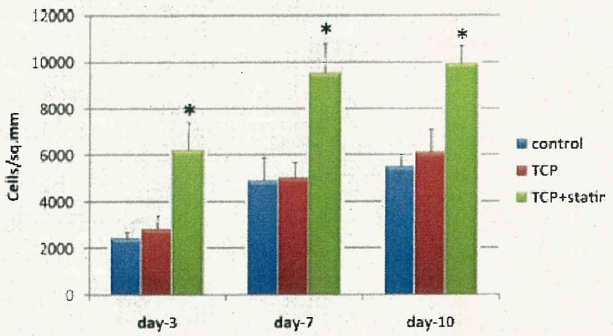

Figure 5. Cell density in the defect region at the middle of the bone defects of control, TCP and simvastatin-αTCP combination groups at day 3, 7, and 10. Values were shown as mean ± SD, $n = 6$. *$p <$ 0.01 compared with control and TCP groups at corresponding time point. [Color figure can be viewed in the online issue, which is available at www.interscience.wiley.com.]

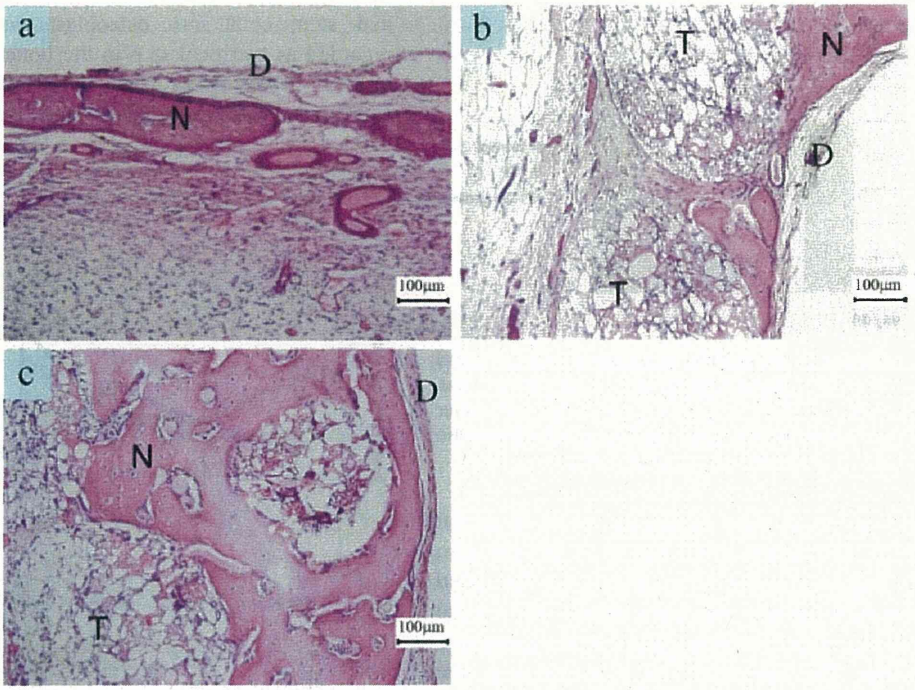

Figure 6. Photomicrographs of the calvarial defects at day 14 representing middle of the bone defects of (a) control (b) TCP and (c) simvastatin-αTCP combination groups. D, dura mater; T, αTCP particles; N, newly formed bone. [Color figure can be viewed in the online issue, which is available at www.interscience.wiley.com.]

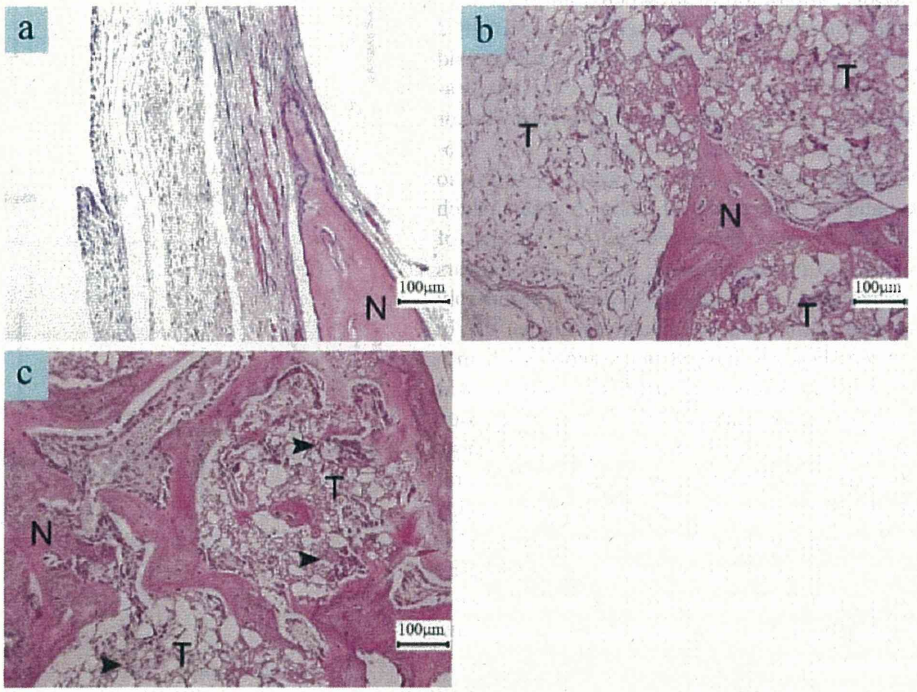

Figure 7. Photomicrographs of the calvarial defects at day 21 representing middle of the bone defects of (a) control (b) TCP and (c) simvastatin-αTCP combination groups. Arrow heads denote proliferating osteogenic cells. T, αTCP particles; N, newly formed bone. [Color figure can be viewed in the online issue, which is available at www.interscience.wiley.com.]

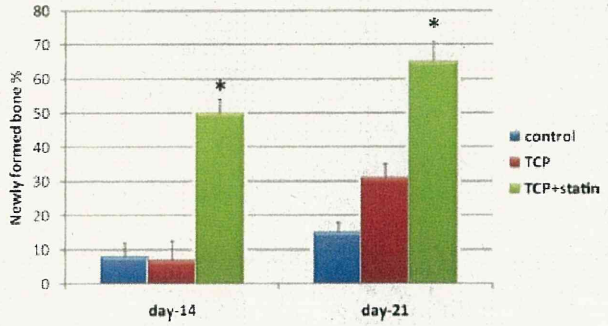

Figure 8. Comparison of new bone area between control, TCP, and simvastatin-αTCP combination groups at day 14 and day 21. Values were shown as mean ± SD, $n = 6$. $^*p < 0.01$ compared with other groups at the same time point. [Color figure can be viewed in the online issue, which is available at www.interscience.wiley.com.]

The results of our *in vitro* experiment showed an initial burst release of simvastatin from αTCP. A similar pattern of release is expected in the bone defect and the released simvastatin would induce the dura mater for cytokine secretion and precursor cells stimulation at the initial phase of bone healing. This appears to be a critical step in the early stage of bone healing providing osteogenic cells which were recruited in the spaces between αTCP particles and between the particles and the dura mater by day 10.

Real-time PCR analysis revealed significantly augmented upregulation of BMP-2 at day 3 in simvastatin-αTCP combination group. It has been reported that BMP-2 stimulates chemotatic migration of mesenchymal progenitor cells and stromal osteoblasts.[25,26] Upregulation of BMP-2 at day 3 would be attributed to the initial migration and recruitment of osteogenic cells from dura mater in simvastatin-αTCP combination group. Transforming growth factor beta (TGF-β) is involved in fracture repair and it is produced by degranulated platelets after initial injury and also by osteoblasts and chondrocytes at later stages, which enhances the proliferation of these cells as well as that of mesenchymal cells and preosteoblasts.[27] TGF-β also appears to stimulate osteoblast proliferation, which presumably increases the pool of committed osteoblast precursors.[28,29] In addition, it has been shown to have strong osteoblast chemotatic effect.[30] In our experiment, TGF-β1 expression was highly upregulated in simvastatin-αTCP combination group at day 7, reaching peak at day 10 and maintained the high expressions until day 14. Histologically, extensive proliferation and migration of osteogenic cells were observed at day 7 and day 10, and continued, albeit to a less extent, at day 14 and day 21. These data suggest that TGF-β1 would play a role in early proliferation of osteogenic cells and continued proliferation and migration of osteoblasts in simvastatin-αTCP combination group.

At day 14, extensive differentiation of recruited cells to osteoblasts and active formation of new bone were evident in the simvastatin-αTCP combination group. Although pre-existing osteoblasts may be involved in the bone repair to some extent, the differentiation of pluripotential mesenchymal stem cells into osteoblasts and chondral cells is regarded as a critical step in the bone healing.[31] Expression of BMP-2 was upregulated significantly at day 14 and its expression was maintained until day 21 in simvastatin

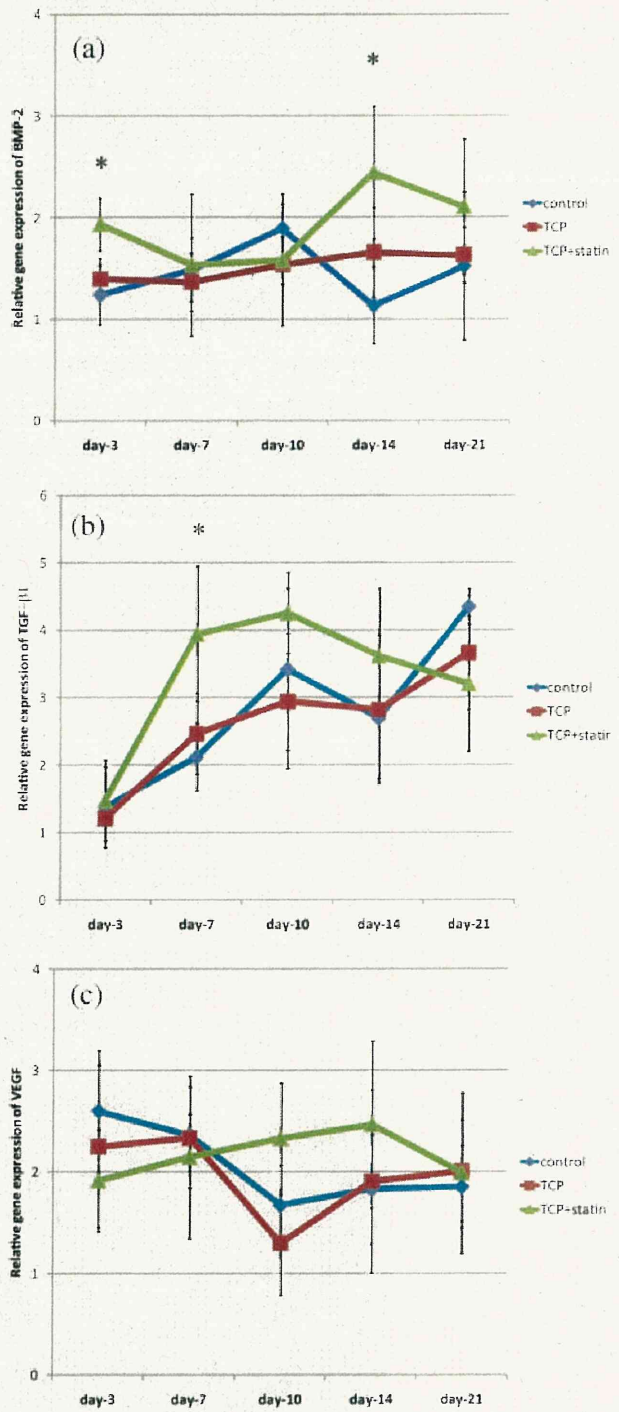

Figure 9. mRNA expression of (a) BMP-2, (b) TGF-β1 and (c) VEGF genes at different time points. Values were shown as mean ± SD, $n = 6$. $^*p < 0.05$ compared with other groups at the same time point. [Color figure can be viewed in the online issue, which is available at www.interscience.wiley.com.]